

Proceedings of GT2006
ASME Turbo Expo 2006: Power for Land, Sea and Air
May 8-11, 2006, Barcelona, Spain

GT2006-90730

THE EFFECT OF LIQUID-FUEL PREPARATION ON GAS TURBINE EMISSIONS

Sosuke Nakamura¹, Vince McDonell and Scott Samuelsen

UCI Combustion Laboratory
University of California, Irvine, 92697-3550

ABSTRACT

The emissions of liquid-fuel fired gas turbine engines are strongly affected by the fuel preparation process that includes atomization, evaporation and mixing. In the present paper, the effects of fuel atomization and evaporation on emissions from an industrial gas turbine engine were investigated. In the engine studied, the fuel injector consists of a co-axial plain jet airblast atomizer and a premixer, which consists of a cylindrical tube with four mixing holes and swirler slits. The goal of this device is to establish a fully vaporized, homogeneous fuel/air mixture for introduction into the combustion chamber and the reaction zone. In the present study, experiments were conducted at atmospheric pressure and room temperature as well as at actual engine conditions (0.34MPa, 740K) both with and without the premixer. Measurements included visualization, droplet size and velocity. By conducting tests with and without the premixing section, the effect of the mixing holes and swirler slit design on atomization and evaporation was isolated. The results were also compared with engine data and the relationship between premixer performance and emissions was evaluated. By comparing the results of tests over a range of pressures, the viability of two scaling methods was evaluated with the conclusion that spray angle correlates with fuel to atomizing air momentum ratio. For the injector studied, however, the conditions resulting in superior atomization and vaporization did not translate into superior emissions performance. This suggests that, while atomization and the evaporation of the fuel are important in the fuel preparation process, they are of secondary importance to the fuel/air mixing prior to, and in the early stages of the reaction, in governing emissions.

NOMENCLATURE

D_{32}	=	Sauter Mean Diameter, m
d_o	=	liquid discharge orifice diameter, m
σ	=	surface tension, kg/s ²
U_R	=	relative velocity (coflowing)
ρ_A	=	density of air, kg/m ³

ALR	=	atomizing air to liquid mass flow ratio
μ_L	=	liquid viscosity, kg/m s
ρ_L	=	liquid density, kg/m ³
L_{premixer}	=	premixer length, m
Re	=	Reynolds number
M	=	Mach number
St	=	Stokes number
LPP	=	Lean Premixed Prevaporized

INTRODUCTION

To meet increasingly stringent emissions regulations, combustors for the next generation of advanced gas turbine engines are being designed to reduce pollutant formation while maintaining efficient performance. In order to achieve low emissions combustion, many strategies are being considered. One strategy that is now common is the use of lean premixed combustion for gaseous fuels.^{1,2} By operating under well mixed and at lean conditions, reaction temperatures can be reduced both locally and on average. For liquid fired systems, achieving low emissions requires not only sufficient mixing of fuel vapor and air, but also sufficient time for atomization and vaporization. If liquid droplets enter the reaction zone, combustion of the vapor produced by these droplets can take place near stoichiometric conditions depending upon the local conditions.³ As a result, the preparation of the fuel/air mixture for liquid fired systems is inherently more complicated than it is for gaseous fuels.⁴

Operating fuel lean, with prevaporized fuel and premixing with air (LPP), has demonstrated low emission levels.^{1,5,6} LPP involves the introduction of a uniformly lean mixture of fuel vapor and air into the combustor. There are several investigations about evaporation and mixing of liquid fuel in LPP system.^{5,7,8} The process in the present system is typical of LPP systems and involves several relatively discrete steps—a twin-fluid atomization approach, followed by vaporization and mixing. Twin-fluid atomization is commonly used in gas turbine applications to enhance mixing and the production of fine droplets with relatively low liquid pressure drops.^{9,10} The rate of vaporization/mixing is

¹ Visiting Scientist, Mitsubishi Heavy Industries, Ltd., Hyogo Japan.

determined largely by the enthalpy and fluid mechanics of the combustion and swirl air.

The study of spray phenomena for gas turbines is challenging due to the difficulties with acquiring information at engine conditions. Droplet size distribution, velocity, evaporation are critical for fuel-air mixing inside combustor, but it is difficult to investigate these characteristics at actual engine conditions. As a result, it is common to conduct measurements in lower pressure and non-reacting test rigs. However, many aspects of the behavior of spray at lower pressure condition may not be representative of the behavior in the engine. Literature regarding scaling methods for two-phase phenomenon in gas turbine combustion is sparse, but work describing strategies for identifying operating conditions that enable measurements at low pressure and temperature while conserving certain flow quantities such as momentum ratio, pressure loss, Re , M , or St can be found.^{11,12,13,14,15} To date, no studies that systematically explore the relative behavior of atomization, vaporization, and mixing at engine conditions and relates that to emissions performance has been conducted. As a result, the current study has been undertaken.

The objective of the present study is to relate the atomization, vaporization, and mixing phenomena occurring within a fuel injector/premixer assembly to emissions performance of a small gas turbine operated on DF-2 (Diesel Fuel #2).

APPROACH

The overall approach taken in the present study to accomplish the objectives is as follows:

- Select an injector that is suitable to meet the objective of the present study.
- Characterize the emissions produced by the gas turbine engine operating at baseline conditions and at conditions where the atomization is systematically varied
- Characterize the spray produced by the engine fuel injector in the absence the premixer hardware under engine and scaled conditions
- Characterize the spray produced by the engine injector/premixer assembly under engine and scaled conditions
- Analyze the results and assess the relative roles of atomization, vaporization, and mixing in the emissions performance
- Analyze the results to evaluate the relative merit of difference scaling strategies for the injector operation in producing “engine like” behavior.

EXPERIMENT

Injector

The injector selected for this study (Figure 1) is the fuel atomizer/premixer assembly used in the Capstone Turbine Corporation C30 microturbine generator (MTG). The injector was selected because the configuration of atomizer is very simple. Figure 1 also illustrates a mechanistic

representation of the spray phenomena that occur within the assembly and are the basis for the objectives of the study.

The premixer has a length $L_{premixer}$, which is the length the atomized fuel droplets have to vaporize and mix with air before they are reacted. The residence time $t_{residence}$ and evaporation time t_{vap} are key parameters that determine the extent to which the fuel has vaporized prior to entry into the combustion chamber. The spray is produced by air-blasted plain jet atomizer that features centerline injection of a liquid column surrounded by a coflowing high velocity annulus of air. The premixer incorporates a radial swirler to help aid in mixing and distributing the spray. Air is added through four round orifices around the atomizer to provide for combustion downstream of the injector as well as to improve mixing. Each air stream can potentially play an important role in the preparation of the fuel/air mixture and therefore influence the formation of pollutants in the gas turbine combustor. The swirl and mixing air are referred to as “Combustion air”.

Injector experiments were carried out on two test rigs, each of which is described briefly in this section.

Fig 1: MTG (Micro Turbine Generator)

The first test rig is the recuperated Model C30 liquid fired microturbine generator. The gas turbine is shown in Figure 2. Capstone C30 Microturbine Generator which shows a photograph of the integrated gas turbine/recuperator along with a cross section through the combustor in a plane perpendicular to the engine shaft. The plane shown cuts through the three fuel injectors which introduce fuel and air tangentially into the combustor.

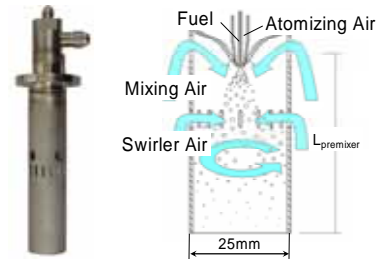


Figure 1. Liquid Atomizer/Premixer Assembly

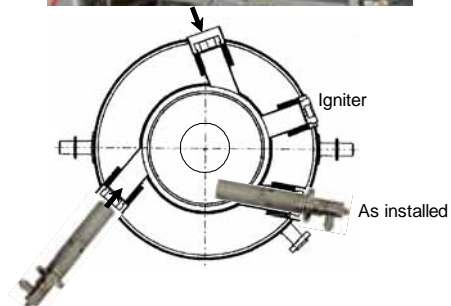


Figure 2. Capstone C30 Microturbine Generator

MTG Instrumentation

The MTG was retrofitted with additional instrumentation to monitor conditions inside the fuel injector. One of the three injector assemblies was fabricated to allow the connection of pressure (pressure transducers) and temperature (thermocouple) measuring devices near the airblast nozzle exit of the injector during operation. The instrumented assembly is shown in the lower left corner of the picture of MTG in Figure 2. Data obtained with this instrumentation was used to establish the conditions to simulate in performing atomization studies of a single injector. And also additional air line was added in order to make it possible to increase atomizing air flowrate.

Emissions Monitoring

Exhaust emissions were measured with a Horiba PG 250 emissions analyzer via an extractive sample probe centered at the exit plane of the exhaust stack. Due to the recuperator, the products of combustion emitted were completely mixed and were highly uniform across the exhaust stack. Emissions were characterized for 50-100 percent load operating conditions. The accuracy of the measurements is ± 0.25 ppm NO_x and ± 2 ppm CO based on instrument specification. The analyzers were zeroed and spanned before and after each measurement campaign and revealed negligible drift and bias.

Rig 2: High Pressure Atomization Test Rig

Experiments were conducted in a facility designed to produce conditions found in conventional and advanced aero-engine combustors. A picture of facility is shown in Figure 3 and is described in more detail elsewhere.^{16,17,18} The pressure vessel and window arrangement used is designed to withstand actual engine conditions. The test section (described below) is mounted centered within the main pressure vessel as shown and injects downward at a plane where various optical ports are available. The entire vessel is suspended from a 2-D horizontal traverse system that allows diagnostics to be fixed to minimize alignment issues. A seal block located at the center of the top flange allowed vertical traversing of the test article within the vessel. All motion is monitored by a magnetic pickup and a precision readout. DC motors are remotely controlled from within the facility control room. The system allows positioning to within 0.2 mm.

In the present study, experiments were conducted on two different injector configurations. The first configuration utilized the fuel injector/premixer assembly as shown in Figure 1 and Figure 4. The air box is designed to allow the swirl and mixing air to be admitted into the premixer in a manner similar to that which occurs in the engine. The second configuration consists of the fuel injector atomization elements in the absence of the premixer as shown in Figure 5. This “airblast nozzle only” configuration was implemented to isolate the role of the atomizing air on the atomizer performance.

All atomization tests were conducted by using same fuel as engine, same injector hardware as engine. Comparing the results from the two configurations just described allows the effect of atomizing air and combustion air on atomization and evaporation to be isolated.



Figure 3. High Pressure Facility

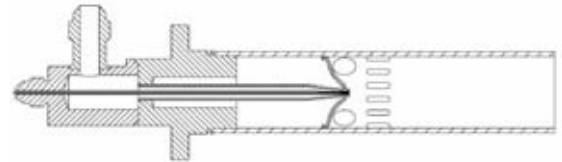


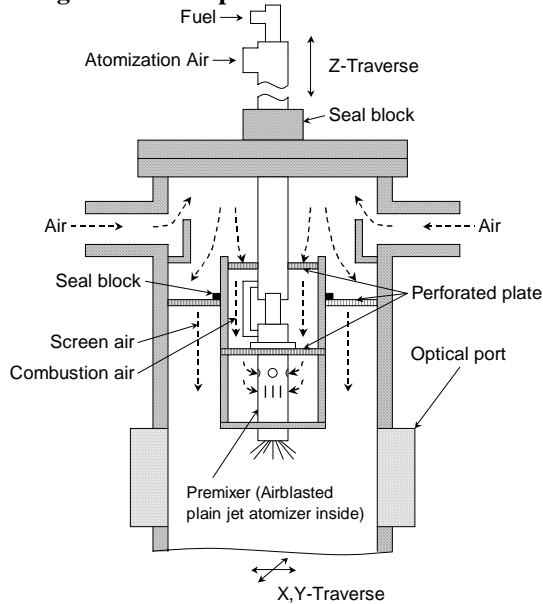
Figure 4. Atomizer/Premixer Assembly



Figure 5. Injector without Premixer Tube

Figure 6 presents details regarding the internal flow distribution of the air for the atomizer/premixer assembly and for the atomizer alone. Since independent control over two preheated air streams was not available, a flow distribution plate was inserted into the chamber (“screen plate”). The plate (1) provides screen air to suppress recirculation of mist back up into the measurement plate and (2) mimics the boundary conditions utilized in the previous studies. Since temperatures at the engine conditions achieved within the high pressure facility were well above the autoignition temperature for DF-2 (~ 500 K¹⁹), nitrogen was mixed into air to weaken the mixture. Nitrogen was added such that the oxygen concentration in screen air, combustion air and atomizing air was reduced from 21% to 9-12% for all tests conditions. Autoignition was not observed during the test campaign.

(a) Rig configuration with premixer



(b) Rig configuration with atomizer only

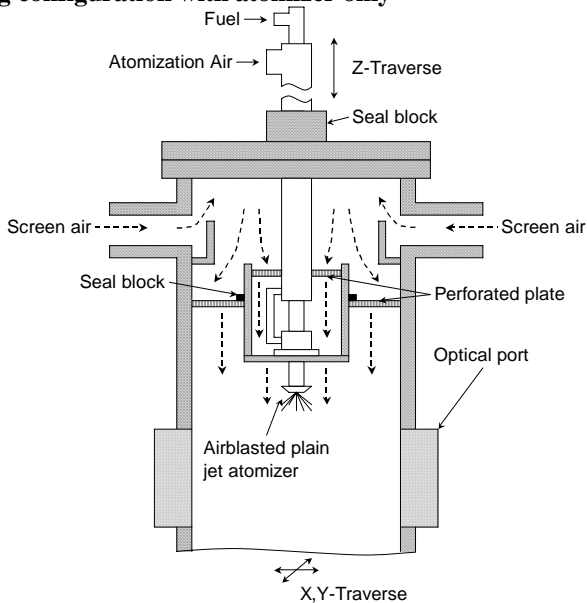


Figure 6. Pressure Vessel Internal Airflow Schematic

Figure 7 presents a cross section of the vessel at the optical access height. 38 mm thick fused silica windows are used to facilitate optical access at the pressures and temperatures of interest for the diagnostics utilized which are described briefly in this section. Internal window cooling/purge was used to maintain the clarity of the windows at the conditions studied.

Phase Doppler Interferometry

Droplet size, radial and axial velocity, volume flux distributions were measured with a two-component phase Doppler interferometer (PDI). A frequency domain processor was used (Aerometrics Model RSA 1000). A fiber optic coupled transmitter was used with 40 mm beam spacing for both sets of beams. A 30-degree forward scatter receiver position was utilized to collect the light refracted by the

droplets. While this angle maximizes signal levels, it does lead to some uncertainty associated with the change in droplet refractive index as the drop temperature increases¹⁸. The uncertainty associated with this effect, however, does not impact the conclusions drawn from the PDI measurements. Measurements were taken for the tests with “atomizer only” at three different locations downstream of the atomizer exit ($Z=25\text{mm}$, 50mm , 75mm).

Visualization

A 1.5 mm thick laser sheet was formed by directing the multi-line beam from a 5W Ar^+ laser into a -6.3 mm focal length cylindrical lens. As shown in Figure 7, the sheet is oriented such that it can intersect the plane containing the injector centerline (the sheet is fixed in space relative to the chamber—such that when the chamber is traversed 75 mm laterally, the sheet will intersect the injector centerline). By recording the scattering of light sheet by the spray, an estimate of the spray evaporation can be obtained. Digital images were obtained at 30 fps with 1/100-1/2000 second exposure times using a Hitachi IEEE-1394 camera (Model KP-D20BU). 100 individual frames from the *.avi file were extracted to *.tif format and then averaged (Media Cybernetics ImagePro Plus Ver. 5.1). In addition, single frame digital images were obtained with a consumer grade 3.2-megapixel camera.

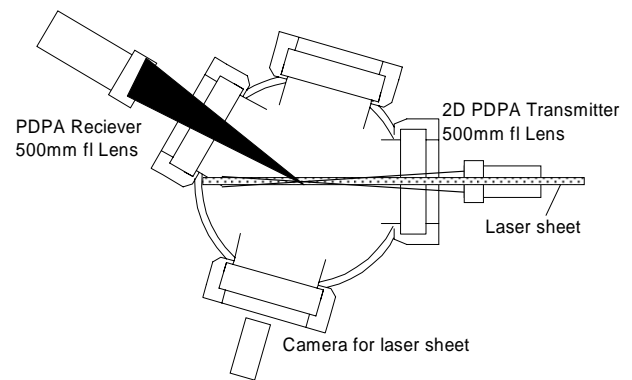


Figure 7. Cross Section at Optical Access Height

Test Conditions

MTG & Atomizer/Premixer Assembly (Phase 1)

All tests were conducted at a condition equivalent to 100% engine load. In addition, the atomizing air to liquid mass flow rates (ALR) was varied from 0.3 to 1.2. Typical engine conditions at 100% are shown in Table 1. All tests carried out in the high pressure vessel were set to same values found in the engine except for the combustion air temperature. The highest pre-mixer inlet temperature that could be attained was 740K.

Atomizer Only Tests (Phase 2)

All tests were carried out at the following conditions shown in Table 2. Tests with high temperature were conducted to isolate the spray characteristics without mixing air and swirler air. Tests with room temperature were to verify scaling method and investigate the pressure effect on atomization.

Table 1. Engine Conditions and Phase 1 Test Conditions

Parameter	Setting
Power Output, kW	25
Combustion Air Press. (MPa)	0.34
Premixer Inlet Temp. in Engine /High Pressure Test Rig (K)	810/740
Atomizing Air Temp. in Engine / High Pressure Test Rig (K)	305/420
$m_{\text{combustion air}}$ (kg/min)	1.82
Primary Equivalence Ratio	0.52
m_{fuel} (kg/min)	0.053
$m_{\text{Atomizing Air}}$ (kg/min)	0.016-0.064
ALR	0.3-1.2

Table 2. Test Conditions for Phase2

Parameter	Setting
Screen Air Press., (MPa)	0.1-0.9
Screen Air Temp. (K)	300, 740
m_{fuel} (kg/min)	0.027-0.184
$m_{\text{Atomizing Air}}$ (kg/min)	0.008-0.064
ALR	0.3-1.2

RESULTS

Baseline Performance of MTG

Emission measurement was obtained for the C30 MTG operated on DF-2 with a set of commercial injectors. Results vs. load setting are presented in Figure 8 for NO and CO emissions. CO emissions decrease with load and are below 10 ppmvd @ 15% O₂ for 50-100% load operation. NO emissions increase with load and are approximately 15 ppmvd @ 15% O₂ at maximum power output. ALR at maximum power output (100% load) is set to 0.3.

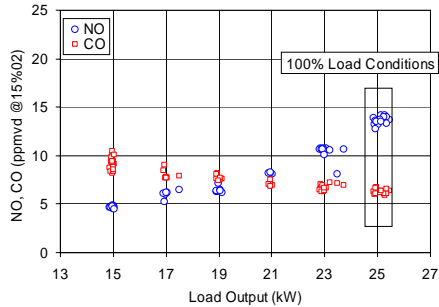


Figure 8. Emission vs. Load Output

To help establish the degree to which the premixer is performing optimally in terms of prevaporizing and premixing the fuel and air prior to entry into the combustor, the baseline emissions measurements were compared to results determined for a “nearly perfect” prevaporized and premixed combustion system.²⁰ Figure 9 shows NO_x as a function of average reaction temperature for the baseline results along with the generalized data obtained for previous mixers (shown by small symbols and black line). The red line shows the estimated data for diesel fuel using data obtained by other workers²². According to the results shown in Figure 8 and Figure 9, it appears that vaporization and mixing in the C30 liquid fuel injector can be improved. Note that results for a natural gas fired 60kW MTG operating at similar conditions and with a similar fuel injection approach but with excellent premixing²¹ affirms this opportunity. As a result, an opportunity to improve the emissions performance through an improvement

in the vaporization (e.g., reducing droplet size) and premixing of the injector is apparent.

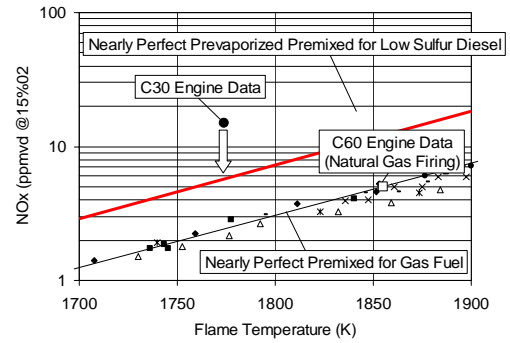


Figure 9. Effects of Nonuniform Fuel and Air Mixing on NO_x Formation²²

Spray Behavior

Uncertainty

An evaluation of spray symmetry and repeatability was carried out to help establish uncertainty in the PDI measurements. Measurements were carried out at 300K and 0.1 MPa in the pressure vessel for two orthogonal traverses at a distance of 25 mm downstream of the injector with fuel flowrate 0.027kg/min and ALR 0.3. The results are shown in Figure 10 which presents error bars based on the differences observed between the two radial profiles obtained. The ratio of volumetric flowrate that is determined by integrating the volume flux profile to metered flowrate of liquid fuel is 0.53-0.86-0.78 for Z=25-50-75mm. The ratio is within experimental uncertainty at 50 and 75mm. At 25 mm, the spray density is high enough to cause some drops to be missed. However, it has been shown that a lack of mass conservation based on flux measurements does not mean measurements of drop size and velocity are incorrect²³. It was observed at higher temperatures and pressures that the symmetry of the spray structure changed somewhat. It is hypothesized that thermal expansion of fuel and atomizing air line at the tip of atomizer alters the spray structure.

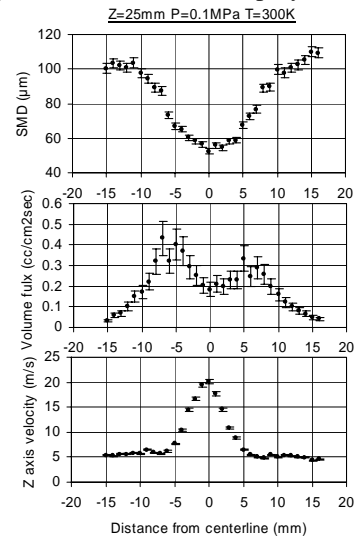


Figure 10. Symmetry Assessment and Uncertainty of Spray Measurement

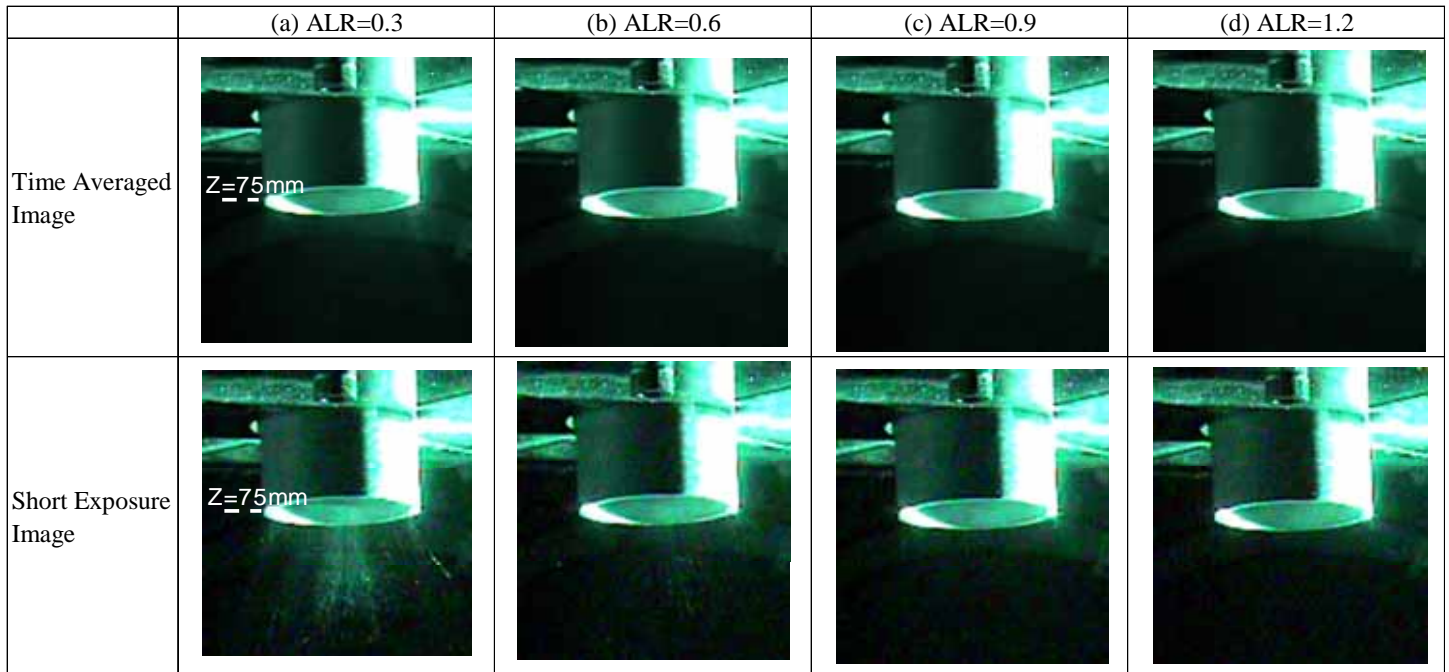


Figure 11. Time Averaged and Short Exposure Laser Sheet Scattering Images at the Exit of Premixer for Actual Engine Condition Cases (Fuel flowrate=0.053kg/min, P=0.34MPa, T=740K)

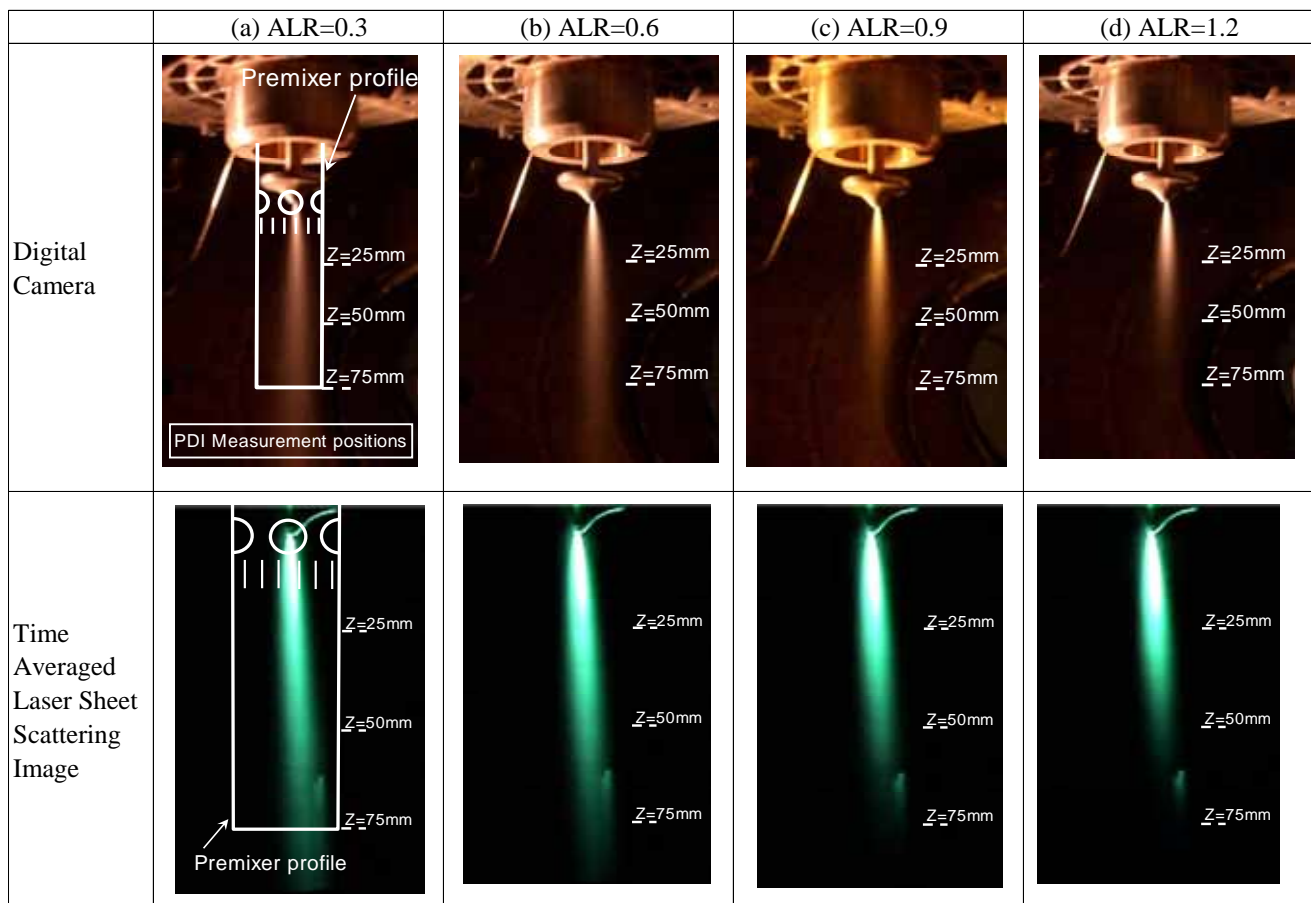


Figure 12. Digital Camera and Time Averaged Laser Sheet Scattering Images of the Spray Plume for Actual Engine Condition Cases (Fuel flowrate=0.053kg/min, P=0.34MPa, T=740K)

Premixer Spray Visualization

Figure 11 presents images of the spray structure obtained from scattering of a laser sheet light in the plane of the centerline of the system at the engine condition (0.34 MPa, 740 K, constant fuel flowrate 0.053kg/min). The 100 frame time averaged images shown in Figure 11 reveal little or no droplet scattering. Careful interrogation of the video images does reveal the presence of some drops at ALR = 0.3 from time to time (e.g., Figure 11 (a)). At higher ALRs, no drops are observed exiting the premixer assembly. This result is interesting in that it suggest that, at the engine condition, some droplets exit the injector prior to complete vaporization.

Spray Behavior in Absence of Premixer

Spray images obtained from scattering of a laser sheet and digital camera at the downstream of atomizer are shown in Figure 12. Images were taken in same manner as described above. As shown in time averaged image of laser sheet scattering and the digital still image (Figure 12 (a)), the droplets are obviously vaporizing as they move downstream. However, for the case corresponding to the engine condition (Figure 12 (a)), it is apparent that droplets are still present at Z=75mm, which is corresponds to the premixer exit plane. Hence, the results observed for the atomizer only correspond well with the results for the atomizer/premixer assembly. In both cases, the results suggest that liquid droplets exit the premixer assembly at engine conditions. This could be a source of the NO_x observed in excess of the perfect mixing case shown in Figure 9.

PDI measurements of droplet size (presented as Sauter Mean Diameter, D_{32}), volume flux (volume of liquid passing through the interferometric probe volume cross section per unit time) and velocity vectors are presented in Figure 13 to Figure 15, respectively.

Figure 13 presents radial profiles of the droplet size distribution D_{32} . As mentioned above, due to thermal expansion of fuel and atomizing air line, the radial profiles are not symmetric, but still provide some important insight into the characteristics of the spray. It is worth noting that the change in symmetry at engine conditions was observed visually as well as in the PDI profiles. Hence, the lack of symmetry in the profiles is not a result of measurement anomalies or errors. Compared to Z=25 mm, the profiles at Z=50 and 75mm, an increase in the distribution D_{32} is observed. At the conditions studied (740 K), small droplets rapidly vaporize, leaving a larger proportion of larger drops which therefore increases the D_{32} .

Profiles of volume flux are shown in Figure 14 and again suggest the presence of an asymmetry. The results also reveal that droplets do exist at an axial location corresponding to the exit of premixer (Z=75mm). Furthermore, the results indicate that, as ALR increases, the droplet volume flux decreases.

Hence, at ALR of 1.2, the droplets are smaller and the volume flux of liquid fuel is lower in number when compared with the engine condition (ALR = 0.3).

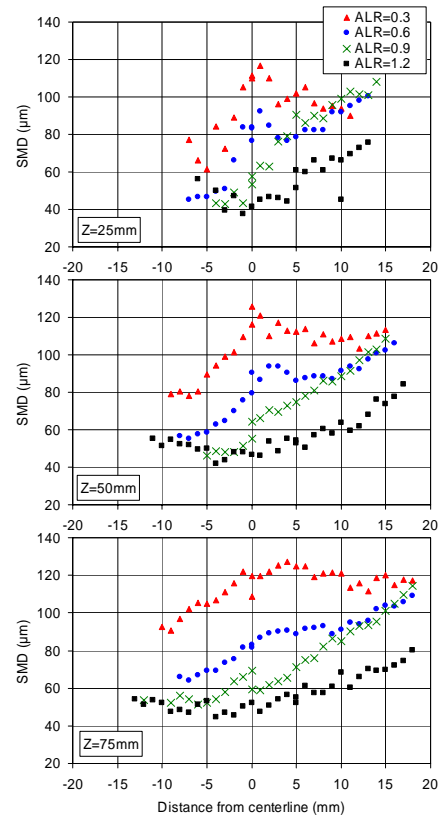


Figure 13. Radial Profiles of D_{32} for Actual Engine Condition Cases

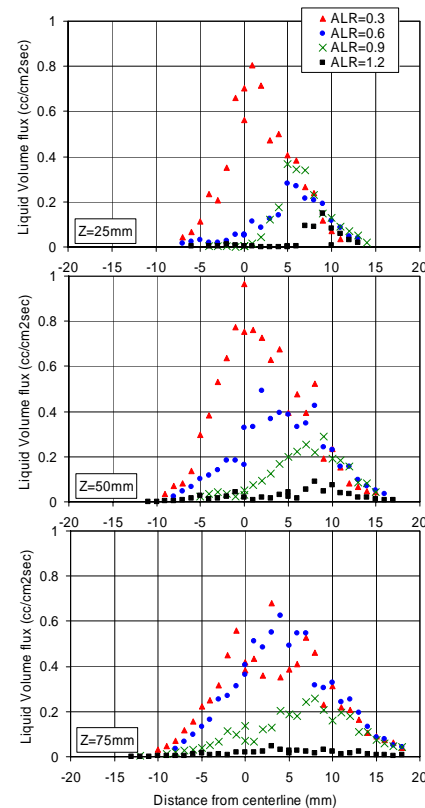


Figure 14. Radial Profiles of Volume Flux for Actual Engine Condition Cases

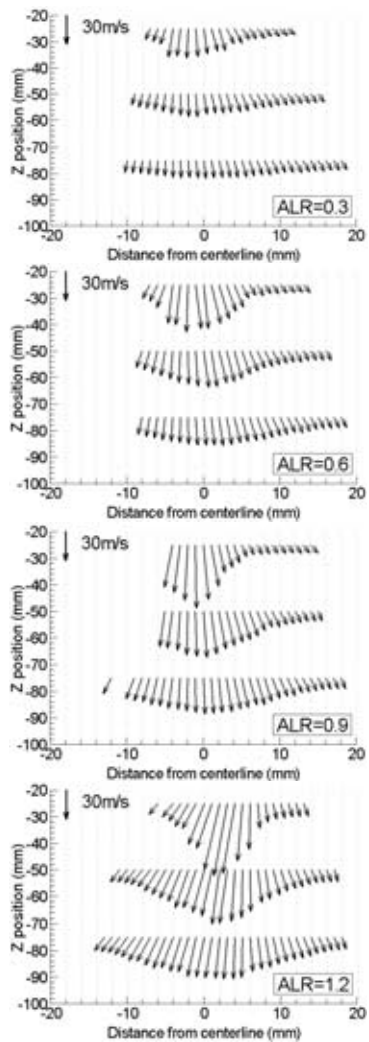


Figure 15. Velocity Vectors in R-Z plane for Actual Engine Condition Cases

Although the results obtained for the spray in the absence of the premixer suggest the presence of drops at 75 mm, the addition of the 740 K swirl and mixing air plays a significant role in the further evaporation of the drops. This is concluded by comparing the results from Figure 11 with Figure 12. Hence, the vaporization characteristics of the spray produced by the atomizer cannot be taken to represent the behavior within the premixer. For example, previous studies suggest secondary atomization due to combustion air may be occurring based on Weber number analysis.²⁴

Influence of Atomizing Air (ALR=0.3-1.2)

Figure 13-Figure 15 also shows the influence of ALR. By changing the ALR, the atomization behavior of the spray can be altered while maintaining the rest of the parameters constant. It is important to note that the atomizing air flowrate is only 1-2% of the total premixer airflow depending upon the ALR used. As ALR increases a number of consistent trends are observed. First, Figure 13 shows that increasing the ALR substantially reduces the droplet sizes. Second, Figure 14 shows that the volume flux is significantly reduced, which is attributed to the smaller droplet sizes. Finally, the axial velocity of the droplets is substantially

higher as ALR increases as shown in Figure 15. Since the D_{32} is lower and axial velocities are higher, vaporization will occur more quickly due to the higher surface area and increased convective mass transfer. As a result, it is not surprising that the volume flux at each axial location is reduced with ALR. This is further corroborated with the visualization results shown in Figure 11.

According to these results, it can be concluded that evaporation and mixing of fuel vapor and air (combustion air = mixing air + swirler air) will be promoted at higher ALR. Given the trends observed with ALR in terms of vaporization and mixing, it is reasonable to expect that the emissions performance (at least NO_x) for higher atomizing air ALRs should be superior when compared to the baseline conditions.

In order to verify the effect of ALR on emissions, ALR was varied at 100% load condition using the MTG with an additional atomizing air circuit added to independently vary atomizing air flow. In the tests, ALR was changed from 0.3-1.2 at constant 100% power output, constant fuel flowrate and constant combustion air flowrate. The results are shown in Figure 16. Interestingly, the results are completely the opposite of the expected tendencies. According to the results from atomization tests, it is considered that higher ALR can promote both evaporation and eventually mixing. But contrary, NO increased with higher ALR. NO emissions are approximately 35 ppmvd @ 15% O₂ at ALR=1.2. CO remains almost constant over the entire range of ALR.

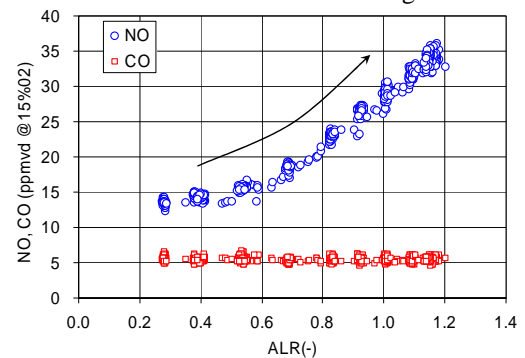


Figure 16. Emission vs. ALR at 100% Load

Possible causes for this non-intuitive behavior are hypothesized as follows. Spray images obtained from the scattering of a laser sheet reveal the presence of a strong recirculation zone one diameter downstream of the premixer (Figure 17), produced by the radial swirler. Therefore, it can be assumed that the flame will be anchored within this region over the entire range of ALR.

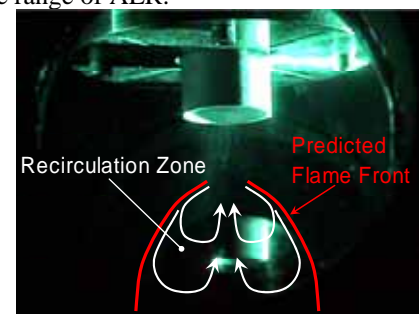


Figure 17. Recirculation Zone downstream of the Premixer

The lower ALR cases have greater residence time (=mixing time) than higher ones due to the difference in droplet velocity as shown in Figure 15, even if droplets are present at the exit of the premixer, sufficient time exists for vaporization and mixing before reaching the flame. On the other hand, the higher ALR cases have shorter residence time than lower ones due to same reason above, even if spray evaporate before reaching the flame, there is not enough time for mixing. Therefore, one possible cause for the NOx increase with higher ALR is that the mixing process is dominated by residence time, and NOx increases with higher ALR due to higher droplet velocities. Another possible cause is that the momentum interaction between fuel spray and combustion leads to locally rich areas with increasing ALR. A computational fluid dynamics (CFD) analysis (using the actual engine configuration and operating conditions) revealed that a rotation of the combustion air occurs in the injector as a result of the tangential introduction of the air. For two reasons, the penetration of the droplets into the rotating combustion air is enhanced at lower values of ALR. First, the droplets are larger and possess, as a result, higher momentum. Second, as the larger droplets penetrate, the interaction with the rotating combustion air further enhances the outward radial velocity. Conversely, at higher ALR, the smaller droplet size constrains the penetration into the combustion air, the core of the mixture exiting the injector is enriched, and the resulting production of NOx is increased.

Evaluation of Scaling Methods

Even though experiments were carried out at actual engine conditions, additional studies were carried out to investigate the viability to two atomization scaling approaches. As a first step, pressure scaling was evaluated. As a result, experiments were carried out at various pressure

conditions in order to simulate droplet size distribution and spray angle. Tests were carried out for the “atomizer only” configuration at room temperature. First, actual engine condition was set as standard condition (P=0.34MPa) and atomizing air and fuel flowrate were changed at each pressure according to scaling strategy. Then the profiles of droplet size were compared with standard condition.

Strategy-1

Since the configuration of the atomizer is similar to plain jet airblast atomizer used to develop the empirical correlation shown in Equation (1),¹ it was considered as a first step to estimate dominant factors controlling spray characteristics especially for D_{32} .

$$\frac{D_{32}}{d_o} = 0.48 \left(\frac{\sigma}{\rho_A U_R^2 d_o} \right)^{0.4} \left(1 + \frac{1}{ALR} \right)^{0.4} + 0.15 \left(\frac{\mu_L^2}{\sigma \rho_L d_o} \right)^{0.5} \left(1 + \frac{1}{ALR} \right) \quad (1)$$

Where

- D_{32} =the Sauter Mean Diameter, m
- d_o =liquid discharge orifice diameter, m
- σ =surface tension, kg/s²
- U_R =relative velocity (coflowing)
- ρ_A =density of air, kg/m³
- ALR=air to liquid mass flow ratio, -
- μ_L =liquid viscosity, kg/m s
- ρ_L =liquid density, kg/m³

Tests were carried out in room temperature therefore thermal property of liquid fuel can be assumed to be identical at each pressure with the assumption of its incompressibility.

According to Equation (1), conserving $\rho_A U_R^2$ and ALR (which is equivalent to conserving the initial kinetic energy of the atomizing air), should result in the same D_{32} .

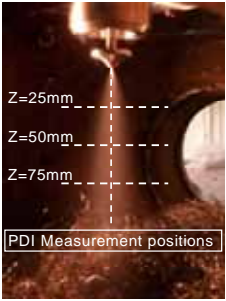






(a) 0.1MPa	(b) 0.3MPa	(c) 0.3MPa	(d) 0.34MPa
			
(e) 0.5MPa	(f) 0.7MPa	(g) 0.9MPa	Fuel Flowrate (kg/min):
			(a) 0.027 (b) 0.039 (c) 0.050 (d) 0.055 (e) 0.071 (f) 0.092 (g) 0.117

Figure 18. Digital camera images at the exit of atomizer for Strategy-1 at different pressure (0.1-0.9MPa) 300K cases

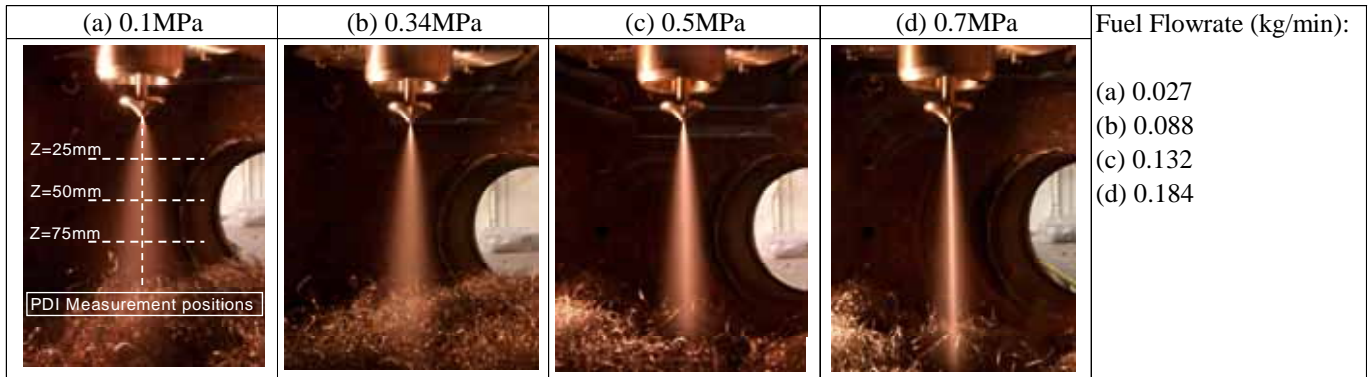


Figure 19. Digital camera images at the exit of atomizer for Strategy-2 at different pressure (0.1-0.7MPa) 300K cases

Strategy-2

The second strategy involved increasing atomizing air flowrate to maintain the ratio of set pressure to standard pressure. This method was established in order to keep the momentum ratio of atomizing air and screen air constant so that spray angle was considered to be same as standard condition. ALR was also conserved.

Figure 18 and Figure 19 show still images of the spray obtained by digital camera. The results shown in Figure 18 and Figure 19 can provide a quantified comparison of spray angle. Figure 20 shows a typical image of spray at 0.1MPa along with a representation of the spray angle measurement procedure. A line profile was drawn across the image at axial distance corresponding to 25mm downstream of atomizer. Then a line was drawn intersecting the center at the exit of the atomizer and the location on the line profile at which the intensity value was found to be saturated. The same process was repeated on the other side of the spray, and the included angle between the two lines is considered to be the spray angle.

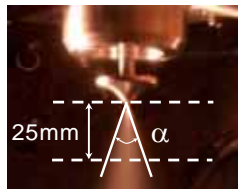


Figure 20. Typical image of spray angle measurement technique

It is observed that the spray cone exhibits a systematic collapse with higher pressure. This tendency can be observed in previous work using an air blast simplex nozzle.¹ According to their work, spray angle correlates with fuel to atomizing air momentum ratio. Figure 21 shows plots of spray angle at 25mm downstream plotted against fuel to air momentum ratio. In the present study, when matching momentum and ALR (Strategy 1), at higher pressure the atomizing air flowrate is increased to keep $\rho_A U_R^2$ constant. However, in order to keep ALR constant, the fuel flowrate was also increased. Therefore, the fuel to atomizing air momentum ratio was increased. Because of relative effect of $\rho_A U_R^2$ and ALR on fuel to atomizing air momentum ratio, this strategy doesn't predict spray angle behavior correctly. The

same basic phenomenon occurs when considering the second scaling strategy as well.

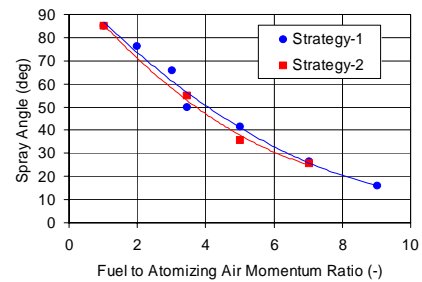


Figure 21. Spray angle measured downstream of the atomizer as a function of fuel to air momentum ratio

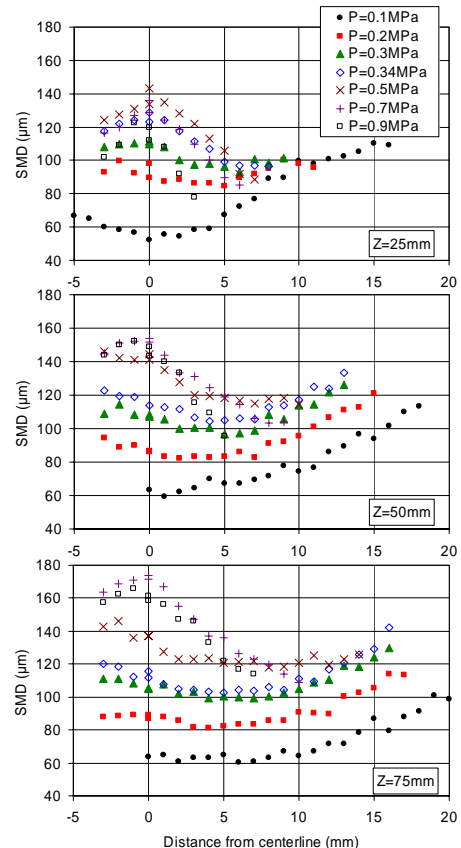


Figure 22. Radial Profiles of D_{32} for Strategy-1

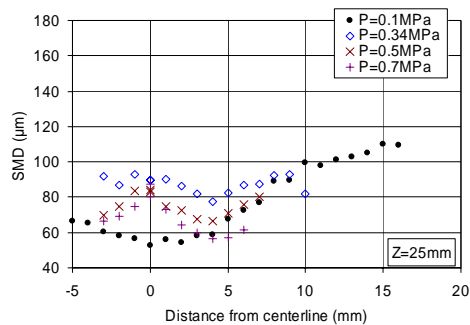


Figure 23. Radial Profile of D_{32} for Strategy-2

Figure 22 and Figure 23 present the radial profiles of D_{32} for each strategy. The radial profiles included data from a few points beyond the centerline as a check on symmetry. These tests were carried out in room temperature hence asymmetry due to thermal expansion is not observed.

The droplet size distribution and spray angle did not match the results obtained at engine pressures ($P=0.34\text{MPa}$) using either strategy. For ambient pressures above 0.2MPa , a local peak in droplet size is evident at the centerline at $Z=25, 50, 75\text{mm}$ corresponding to poor atomization of the central liquid core. At 0.1MPa the profile reveals a local minimum at the centerline and local maximums at the extreme edge of the spray.

CONCLUSIONS

This study represents the first documented investigation between fuel preparation and emissions at actual engine conditions by using a practical injector in both a controlled, well instrumented, laboratory test rig and in a practical gas turbine engine. The performance of a fuel injector in preparing the fuel/air mixture for combustion was investigated in the laboratory at actual engine conditions using PDI and flow visualization. The emissions produced by a commercial microturbine generator operating with this same injector at the same condition studied in the laboratory. In the laboratory, two strategies for scaling the atomization from 0.1MPa to 0.9MPa were evaluated. One strategy was to match $\rho_A U_R^2$ and ALR, and the second strategy was to keep the momentum ratio of atomizing air and screen air constant. Conclusions drawn from the study are as follows:

- For the range of pressures and temperatures studied, the spray angle for the air blasted plain jet injector used correlates well with fuel to atomizing air momentum ratio, a useful result for combustor and injector designers concerned with affecting spray angle as a strategy in the fuel preparation process.
- At engine combustor inlet conditions, the vaporization rate observed for the complete injector/premixer assembly is comparable to that for the spray with atomizing air alone. As a result, it may be reasonable to estimate evaporation rates based strictly on atomization process in the present case.

- Observations in the laboratory that would normally be expected to lead to a reduction in NO emission produced, in fact, a higher emission of NO in the practical engine. For example, higher ALR was found in the laboratory injector studies to markedly reduce droplet size and increase vaporization rates with the expectation of improved homogeneity of the resultant fuel/air mixture, but to produce higher NO emission from the practical engine. This implies that a design strategy focused on improving atomization of the spray such that no droplets exit the premixer is not sufficient to infer emissions performance. Indeed, in the present case, emissions were minimized at a condition that was observed to result in droplets exiting the premixer. It is inferred that, in advanced injector designs, the emissions are likely dictated by the fuel/air mixture properties (e.g., temporal and spatial distribution of homogeneity) prior to and within the primary zone of stabilization.
- In practical hardware, the homogeneity of the mixture exiting the injector is a complex marriage of mixing between the fuel and the combustion air. Factors contributing to the homogeneity include atomization, evaporation, droplet momentum and thereby droplet penetration. Such processes are undoubtedly dependent on injector design and vary from injector to injector. For the Capstone C30, the ALR is optimally set for (1) emissions, (2) stability, and (3) coking.
- Simply reducing drop size will not necessarily result in superior emission performance.

ACKNOWLEDGEMENTS

The authors acknowledge the support of the California Energy Commission (Contract 500-00-020), Mitsubishi Heavy Industries, and Capstone Turbine Corporation. The authors would like to acknowledge the great contributions of University of California, Irvine Combustion Laboratory (UCICL) staff and students including Mr. Richard Hack, Mr. Josh Mauzey, Mr. Christopher D. Bolszo, Mr. Brandon J. Masuda, Mr. Steven R. Hernandez, Mr. Nikhil K. Kar, Mr. Patrick M. Couch and Mr. Peter L. Therkelsen for assistance with the preparation and operation of test facility.

REFERENCES

- ¹ Lefebvre, A.H. (1999). *Gas Turbine Combustion*, 2nd Edition, Taylor & Francis, Philadelphia.
- ² Richards, G.A., McMillian, M.M, Gemmen, R.S., Rogers, W.A., and Cully, S.R. (2001). Issues for low-emissions, fuel flexible power systems, *Prog. Energy and Comb Sci*, Vol. 27, pp. 141-169.
- ³ Chiu, H.H. and Liu, T.M. (1977). Group combustion of liquid droplets, *Comb Sci Tech*, Vol. 17, pp. 127.
- ⁴ Lefebvre, A.H. (1995). The role of fuel preparation in low-emission combustion. *J. Engr Gas Turbines and Power*, Vol. 117, pp. 617-654.
- ⁵ Behrendt, T. Heinze, J. and Hassa, C. (2003). Experimental investigation of a new LPP injector concept for

aero engines at elevated pressures, Paper GT2003-38444, Turbo Expo 2003, Atlanta.

⁶ Zaralis, et al. (2002). Low NOx Combustor Development pursued within the scope of Engine 3E German national research program in a cooperative effort among engine manufacturer MTU, University of Karlsruhe and DLR German Aerospace Research Center, *Aerospace Science and Technology*, Vol. 6, No. 7, pp. 531-544.

⁷ Becker, J., Hassa, C. (2003), Liquid fuel placement and mixing of generic aeroengine premix module at different operating conditions (2003), *ASME J. For Gas Turbines And Power* Vol. 125, pp. 901-908.

⁸ Rachner, M., Brandt, H. E. and Hassa, C. (1996), A numerical and experimental study of fuel evaporation and mixing for lean premixed combustion at high pressure (1996), *Twenty-fifth Symposium (International) on Combustion*, Vol. 2, pp. 2741-2748.

⁹ Lefebvre, A.H. (1998). *Atom and Sprays*, Hemisphere Publishing.

¹⁰ Georjon, T.L., and Reitz, R.D., *Atom and Sprays* 9:231-254 (1999).

¹¹ Jermy M.C., Hussain M. and Greenhaigh D.A. (2003), Operating liquid-fuel airblast injectors in low-pressure test rigs: strategies for scaling down the flow conditions (2003), *Meas. Sci. Technol.* Vol. 14, pp. 1151-1158.

¹² Sayre A.N., Dugue J., Weber R., Domnick J. and Lindenthal A. (1994), Characterization of semi-industrial-scale fuel-oil spray issued from a Y-jet atomizer, *J. Inst. Energy*, Vol. 67, pp. 70-7.

¹³ Mcvey J.B., Kennedy J.B. and Russell S. (1989), Application of advanced diagnostics to airblast injector flows, *J. Eng. Gas Turbines Power*, Vol. 111, pp.53-62.

¹⁴ Lefebvre, A.H. (1998). *Atom and Sprays*, Hemisphere Publishing.

¹⁵ Wang, H.Y., McDonell, V.G., Sowa, W.A., and Samuelsen, G.S. (1993). Scaling Of The Two-Phase Flow Downstream Of A Gas Turbine Combustor Swirl Cup: Mean Quantities (1993). *ASME J. For Gas Turbines And Power* Vol. 115, pp. 453-460.

¹⁶ Leong, M.Y., McDonell, V.G. and Samuelsen, G.S. (2001). Effect Of Ambient Pressure On An Airblast Spray Injected Into A Crossflow (2001). *J. Prop. And Power*, Vol. 17, No. 5, pp. 1076-1084.

¹⁷ Leong, M.Y., Smugeresky, C.S., McDonell, V.G., and Samuelsen, G.S. (2001). Rapid Liquid Fuel Mixing For Lean Burning Combustors: Low Power Performance (2001). *ASME J. Engr. Gas Turbines And Power*, Vol. 123, pp. 574-579.

¹⁸ McDonell, V.G., Seay, J.E., and Samuelsen, G.S. (1994). Characterization Of The Non-Reacting Two-Phase Flow Downstream Of An Aero-Engine Combustor Dome Operating At Realistic Conditions. Paper 94-GT-263, presented at ASME IGTI Meeting, The Hague, Netherlands, June.

¹⁹ Glassman, I., *Combustion*, 3rd. E., Academic Press: New York, 1996.

²⁰ Leonard, G. and Stegmaier, J. (1994). Development of an Aero-derivative Gas Turbine Dry Low Emission Combustion System, *J. Engr Gas Turbines and Power*, Vol. 116, pp. 542-546.

²¹ Phi, V.M., J.L. Mauzey, V.G. McDonell, and G.S. Samuelsen (2004). Fuel Injection and Emissions Characteristics Of A Commercial Microturbine Generator. Paper GT-2004-54039, Turbo EXPO 2004, Vienna, Austria, June

²² John C.Y. Lee, Philip C. Malte and Michael A. Benjamin (2001), Low NOx Combustion for Liquid Fuels: Atmospheric Pressure Experiments Using a Staged Prevaporizer-Premixer (2001). Paper 01-GT-0081, presented at the 46th ASME IGTI Conference, Louisiana

²³ Edwards, C.F. and Marx, K.D. (1992). Analysis of the Ideal Phase-Doppler System (1992), *Atomization and Sprays*, vol. 2, pp. 319-366.

²⁴ C.D. Bolzso, J.L. Mauzey, V.G. McDonell, and S. Nakamura (2005). Experimental investigation of liquid fuel atomization, mixing and pollutant emissions for a 30 kW gas turbine engine (2005). *Proceedings*, 18th ILASS-Americas Conference, Irvine, CA, May.

²⁵ Lorenzetto, G.E., and Lefebvre, A.H. (1977). Measurements of Drop Size on a Plain Jet Airblast Atomizer, *AIAA J.*, Vol 15, No. 7, pp. 1006-1010.

²⁶ Benjamin, M.J., McDonell, V.G., and Samuelsen, G.S. (1997). Effect Of Fuel/Air Ratio On Air Blast Simplex Nozzle Performance (1997), Paper 87-GT-150, presented at the 42nd ASME IGTI Conference, Orlando